Several Aspects of the Atomization Behavior of Various Newtonian Fluids with a like-on-like Impinging Jet Injector

G. Bailardi*, M. Negri†, H.K. Ciezki‡
DLR – German Aerospace Center
Institute of Space Propulsion
Lampoldshausen, D-74239 Hardthausen, Germany

Abstract

The atomization characteristics of various Newtonian fluids with a doublet like-on-like impinging jet injector under ambient pressure and temperature conditions and jet velocities up to 80 m/s was investigated and compared. It could be observed that with increasing jet velocity the breakup behavior of the investigated fluids changes in different manner. Seven different main breakup modes could be identified and arranged in a Weber-Reynolds regime diagram for Reynolds and Weber numbers from 10^1 to 10^5 and Ohnesorge numbers from 0.0027 to 3.8.

Introduction

Impinging jet injectors are often used for the atomization of storable liquid and gelled fuels and oxidizers in rocket engines due to their simplicity, low manufacturing costs, good atomization and mixing characteristics, etc. (see e.g. Sutton [1]). Since the 50'es of the 20th century a large number of studies were conducted with several Newtonian fluids. Of particular significance was the introduction of the first categorization of observed spray patterns by Heidmann et al [2] and the study with laminar and turbulent jets performed by Dombrowski and Hooper [3]. One of the first important theoretical studies was from Taylor [4] who formulated a theory, which allows a good prediction of the shape of the fluid sheet formed by the impingement of the jets under low velocity conditions. Many other studies followed, focusing on various aspects of the breakup characteristics such as shape and thickness distribution of the sheet (e.g. Refs. [5] and [6]), breakup length (e.g. Ref. [7]), size of droplets formed (e.g. Ref. [8]) and the effects of higher ambient pressure (e.g. Ref. [9]). A very detailed description of physical phenomena underlying the breakup of liquid sheets is given in a series of articles published recently from a group from the University of Provence in France [10]. A very first comparative study about the breakup behavior of different fluids was conducted by Ciezki et al [11] who used some distinct fluids with different viscosity, density and surface tension values so that different atomization regimes were observed by the authors in dependence of various parameters. They could show that these regimes can be arranged in a regime diagram in dependence upon Reynolds and Weber numbers. The objective of the work presented here is to describe the breakup behaviour of a doublet like-on-like impinging jet injector with a distinct geometry more detailed in a wide range of Reynolds (*Re*), Weber (*We*) and Ohnesorge (*Oh*) numbers.

Experimental Setup, Materials and Methods

The experimental setup consists of a cartridge with the fluid to be investigated, a hydraulic driving unit and a modular injector unit (Figure 1). The injector arms of the injector unit are mounted on movable rotary tables so that the impingement angle as well as the pre-impingement length can be varied easily. For the present work an impingement angle (2Θ) of 90° and a pre-impingement length (L_{pr}) of 5 mm have been chosen. The injector tips (nozzles) can easily be changed for the variation of the nozzle exit diameters and the internal injector geometry. The high ratio l/D_{inj} = 10 of the internal injector channel as well as the internal wall inclination angle of α = 20° were chosen both to reduce influences of separation by the formation of a vena contracta, etc. in the intake to the injector channel and to induce a more fully developed velocity profile at the injector exit (Figure 2). For the visualization of the spray patterns the shadowgraph-technique was used, together with two CCD cameras, one parallel and one perpendicular to the plane of the injectors, and two Nanolite spark lights as light sources. An average of more than 50 pictures was determined to ensure stationary conditions for every experiment.

‡ Corresponding author: Head propellants department, mailto: helmut.ciezki@dlr.de
† Research Engineer
* Master degree student from Polytechnic of Milan

For the task to visualize the breakup behavior of the above described impinging jet injector in a wide range of Reynolds, Weber and Ohnesorge numbers 18 fluids were chosen with the specification of cover a broad range of *Oh*. In Table 2 these fluids are listed together with their properties and calculated *Oh* based on the injector exit diameter d_j = 0.7 mm.

The temperature in the test cell was recorded and taken into account for the determination of fluid properties in each experiment. The actual values of viscosity and surface tension at this ambient temperature were calculated by interpolation of data from Refs. [12].

Results and Discussion

Table 1 presents typical shadowgraph images of the atomization of four selected fluids with different *Oh* numbers. For all fluids tested different breakup patterns could be observed with increasing jet velocity, and thus increasing *Re* and *We* numbers. For n-Heptane (left column), which is a fluid with a very low *Oh* number, at low injection velocities (and thus low *Re* and *We*) a flat sheet with a distinct rim is produced perpendicularly to the plane of the two impinging jets. From the rim, which surrounds the whole sheet, droplets are separated in a stochastic manner. Going to higher velocities (and thus higher *Re* and *We*) a flapping motion of the lower part of the sheet breaks up the rim so that the two sides of the rim aren't anymore in contact. The rim disappears completely for further increases in velocity and the sheet becomes ruffled. For the highest presented injection velocities the sheet gets smaller and smaller and the fluid atomizes in droplets very close to the impingement point. Tests with Glycerine (right column), which is a fluid with a very high Oh number, show that the jets do not impinge at lower velocities due to the bending of the jets by gravitation. Increasing the velocity leads to the impingement of the jets and to the formation of a smooth sheet with a distinct thick rim perpendicular to the plane of the jets. The shape of the sheet is very elongated. For further increase in velocity the lower part of the sheet starts to flap. At the higher injection velocities the sheet increases in width. The inner part of the sheet remains smooth up to a distinct bow-shaped line. Downstream (going to the outer region) starts an increasing flapping of the sheet, which leads to a breakup into droplets as can be seen on the lowest image in the column. Furthermore it can be seen that the distinct rim remains up to high velocities in the upper part of the sheet and vanishes not till the breakup region.

Summarizing it can be said that with increasing *Re* different breakups patterns occur. These patterns are not identical for all fluids, but nevertheless similarities can be found. Comparing the obtained images seven different breakup modes could be identified, which are presented in the following. It has to be noted that some of these modes and structures have been described previously, see e.g. Ref. [11].

Breakup modes

Closed Rim (Figure 3): From the impingement point, where the jets collide, the liquid expands radially creating a flat and thin sheet, perpendicular to the jets collision plane, bounded by a distinct and pronounced rim. This rim collects the major portion of the liquid flow as it is described in Ref. [2]. At the lower end of the sheet the two arms of the rim impinge under a distinct angle. At this tip is formed either a single stream, which breakup into droplets, or another smaller sheet normal to the previous one, which may subsequently decay into droplets.

Open Rim (Figure 4): The sheet is not totally surrounded by a distinct rim. A flapping motion of the lower part of the sheet, which is caused by a Kelvin-Helmholtz-type instability (see e.g. Refs. [10, 13]), breaks up the rim and the sheet into ligaments and droplets so that the two arms of the rim aren't anymore in contact. On the side view image it can be seen how this instability generates wavy structures, which lead to the breakup. Also larger droplets could shed from the rim according to the capillary instability effect, see Ref. [10].

Rimless Separation (Figure 5): Distinct rims aren't visible anymore. The rupture of the almost circular liquid sheet starts at the sides with the separation of parts of the sheet in the region of the Kelvin-Helmholtz-type instabilities. A direct shedding of droplets from the sheet always occurs and parts of sheet separate periodically decaying farther downstream.

Smooth Sheet Ligaments (Figure 6): This breakup shows some similarities to the Rimless Separation mode. But instead of the droplet dominated direct sheet decay, a periodic separation of bow-shaped structures (also called ligaments) from the sheet occurs, which subsequently decay into droplets downstream. The separation of these ligaments is supported by the occurrence of holes in the sheet, which grow in size. It seems that these holes appear after the highest amplitude of the wavy structures present on the sheet.

Ruffled Sheet Ligaments (Figure 7): In this mode the inner part of the sheet is not anymore smooth. Wavy structures occur directly on the sheet, which size (in particular the breakup length) is difficult to detect on the images. The bow-shaped ligaments, which are moving periodically downstream, seem to be separated significantly earlier from the sheet so that the sheet size seems to be significantly reduced. Also it can be seen on the side view image that the spreading angle of the droplets is significantly larger than for the smooth sheet ligaments mode.

Fully Developed Breakup (Figure 8): A direct decay into droplets without any ligaments formation seems to occur comparatively near the impingement point of the two jets. The related Reynolds number of this experiment indicates that the state of fluid flow in the injector passages can be assumed as turbulent. Furthermore it can be seen on the shadowgraph image that the separated droplets are mainly concentrated in bow-shaped "clouds", so that waves of droplets spread downstream periodically.

Aerodynamic Instability Breakup (Figure 9): No droplets were separated from the sides of the rims of the liquid sheet at low jet velocities. The sheet is long and narrow and its surface is smooth. At a distinct higher jet velocity the sheet starts to be subjected to an aerodynamic instability that generates a flapping motion of the sheet. The side view presented in Fig. 9 clearly shows this flapping. It should be noticed that the upper part of the sheet remains stable, i.e. a flat sheet with a distinct thick rim. No capillary instabilities could be observed in this region. A more detailed phenomenological explanation is given in Ref. [14].

Regime diagram

The experiments can be positioned in a Reynolds vs. Weber numbers diagram, which is presented in Fig.10. Tests conducted with the same liquid for increasing injection velocities are laying on a straight line in this log-log diagram due to the equation $We = Oh^2 \cdot Re^2$. The Ohnesorge number of the used fluids increases moving form right to left in the diagram in a range from 0.027 (Hexene) to 3.83 (99% Glycerine solution). The data points in the diagram have different symbols and are additionally color-coded to show the respective breakup regime. It can be seen that the Closed Rim (CR) mode occurs for all fluids. It is detectable in the region of $10^2 < Re < 10^4$ below a constant Weber number of approximately We < 300. The low Weber indicates that in this region the surface tension forces are dominant in comparison to the inertial forces for fluids of approx. $Oh < 0.1$. Taylor [3] stated that the surface tension forces are that what holds together the rim, which may be an explanation why distinct rims can be observed in the low *We* region. Moreover in the left part of the diagram (at approx. $Re < 50$), where the liquids with the highest *Oh* are located, the CR regime expands to higher Weber numbers.

The Rimless Separation mode presents the transition between the Open Rim mode and the two modes with ligaments structures (Smooth Sheet and Ruffled Sheet) for fluids with Ohnesorge numbers in the range $0.044 < Oh < 0.25$. This mode occurs in a small band, whose position in the diagram decreases slightly with increasing *Re*. The Smooth Sheet with Ligaments pattern was found above a nearly constant Weber number at approx. $We \approx 4 \cdot 10^3$ in the Reynolds number range from $8 \cdot 10^1$ to $5 \cdot 10^3$. For higher *Re* the Ruffled Sheet with Ligaments structures mode occurs. The different behavior of the sheet for these two ligaments forming breakup patterns may probably be related to the fact that the injector internal flow conditions of the impinging jets are laminar for the Smooth Sheet mode and turbulent for the Ruffled Sheet mode. This agrees with the observation that above a certain *Re* all sheets are ruffled. The Fully Developed Breakup regime is located in the region of highest *Re* and *We*, at approx. $Re > 5 \cdot 10^3$ and $We > 1 \cdot 10^4$. It can be assumed that on the one hand the state of fluid flow in the injector tip passages is turbulent. On the other hand the influence of the surface tension forces is low in comparison to the inertial forces. In the limited region of very low Reynolds (and relatively high Ohnesorge) numbers a breakup pattern, which was called “Aerodynamic Instability Breakup mode”, could be identified for the three liquids with the highest *Oh*. More detailed information is given in Ref. [13] for a better understanding of the governing processes and its similarity with the spray behavior of gelled fluids.

Summary and Conclusion

The atomization behavior of eighteen different Newtonian fluids with a doublet like-on-like impinging jet injector under ambient pressure and temperature conditions was studied and compared. A distinct geometry was chosen for all experiments and the velocity of the impinging jets was varied up to 80 m/s. The properties of the selected liquids together with the variation of the jet velocity in a wide range offered the possibility to conduct experiments in a wide range of dimensionless numbers, i.e. $10^1 < Re < 10^5$, $10^1 < We < 10^5$ and $0.0027 < Oh < 3.8$.

For all fluids tested the breakup behavior changes with increasing jet velocity, and thus increasing *Re* and *We* numbers. Seven different breakup patterns could be identified. A relation between Reynolds, Weber and Ohnesorge numbers and the location of these breakup regimes in a *Re*-*We* regime diagram could be shown for the investigated fluids. Up to now only for some of these breakup modes information about governing processes could partly be given or it could be referred to relevant literature. It is obvious that further investigations are necessary for a better understanding of the governing processes in all breakup modes at ambient pressures but also e.g. at higher pressures and different injector geometries to cover better significant parts of the range of boundary conditions relevant for propulsion applications.

Acknowledgments

The authors would like to thank A. Feinauer for his help during the conduction of the experiments and Prof. L. DeLuca and Dr. O. Haidn for their support.

Nomenclature

D_{inj}	injector exit diameter [mm]	
L_{pr}	pre-impingement length [mm]	
l_{in}	internal channel length [mm]	
Oh	Ohnesorge number [-]	$Oh = \eta/\sqrt{\rho\sigma D}$
Re	Reynolds number [-]	$Re = \rho UD/\eta$
U	velocity [m/s]	
We	Weber number [-]	$We = \rho U^2 D/\sigma = Oh^2 \cdot Re^2$
α	internal wall inclination angle [°]	
θ	impingement half angle [°]	
μ	liquid viscosity [Pa·s]	
ρ	liquid density [kg m^{-3}]	
σ	liquid surface tension [Nm^{-1}]	

References

[1] Sutton, G.P., *Rocket Propulsion Element: An Introduction to the Engineering of Rockets*, John Wiley, NY USA, 1992, pp.298-311.
[2] Heidmann, M.F., *A Study of Sprays Formed by Two Impinging Jets*, NACA TN 3835, 1957.
[3] Dombrowski, N., and Hooper, P.C., *A study of the Sprays Formed by Impinging Jets in Laminar and Turbulent Flow*, J. Fluid Mechanics, Vol.18, Part 3, 1963, pp. 392-400.
[4] Taylor, G.I., *Formation of Thin Flat Sheets of Water*, Proc. Roy. Soc. A, 259, 1960, pp. 1-17.
[5] Ibrahim, E.A., and Przekwas, A.J., *Impinging Jet Atomization*, Phys. Fluids Vol. 3, No. 12, December 1991, pp. 2981-2987.
[6] Hasson, D. and Peck, R.E., *Thickness Distribution in a Sheet Formed by Impinging Jets*, AIChem Journal, September 1964, pp 752-754.
[7] Anderson, W.E, Ryan, H.M., Pal, S. and Santoro, R.J., Fundamental *Studies of Impinging Liquid Jets*, AIAA 92-0458, 1992.
[8] Anderson, W.E, Ryan, H.M., Pal, S. and Santoro, R.J., *Atomization Characteristics of Impinging Liquid Jets*, Journal of propulsion and Power, Vol.11 No.1, pp.135-145, Jan-Feb, 1994.
[9] Jung, K., Lim, B., Khil, T., and Yoon, Y., *Breakup characteristics of laminar and turbulent liquid sheets formed by impinging jets in high pressure environments*, AIAA 2004-3526, 11-14 July 2004, Florida
[10] Bremond, N., and Villermaux, E., Atomization by jet impact, J. Fluid Mech., vol.549, pp. 273-306, 2006.
[11] Ciezki, H.K., Tiedt, T., von Kampen, J. and Bartels, N., *Atomization Behavior of newtonian Fluids with an Impinging Jet Injector in Dependence upon Reynolds an Weber Numbers*, AIAA 2005-4467.
[12] Lide, D. R., Handbook of Physic and Chemistry, 83rd ed., 2002.
[13] Heislbetz, B., Madlener, K. and Ciezki, H.K., "Breakup Characteristics of a Newtonian Liquid Sheet formed by a Doublet Impinging Jet Injector," AIAA-2007-5694, 43rd Joint Propulsion Conference, Cincinnati, Ohio, USA, 2007.
[14] Negri, M., Bailardi, G., and Ciezki, H.K., *Phenomena Associated with the Breakup of Sheets formed by Newtonian and non-Newtonian Fluids in an Impinging Injector*, Spray 2010 Workshop, Heidelberg, Germany, 3-5 May 2010.

Weber	**n-Heptane** ***Oh* = 0.0040**	**Ethanol** ***Oh* = 0.0097**	**1-Octanol** ***Oh* = 0.078**	**98% Glycerine** ***Oh* = 3.83**
>200	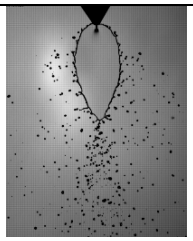 *Re*=1349 U_{jet}=1.3m/s	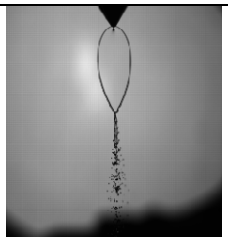 *Re*=828 U_{jet}=2m/s	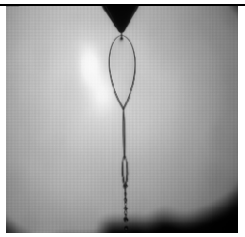 *Re*=189 U_{jet}=2.6m/s	NO IMPINGE MENT
700 ÷ 800	 *Re*=7137 U_{jet}=6.5m/s	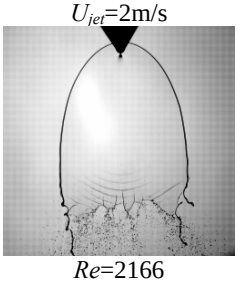 *Re*=2166 U_{jet}=5.2m/s	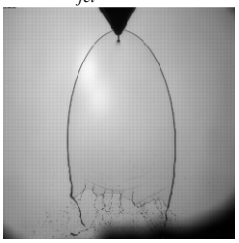 *Re*=378 U_{jet}=5.2m/s	 *Re*=6 U_{jet}=6.5m/s
2000 ÷ 3000	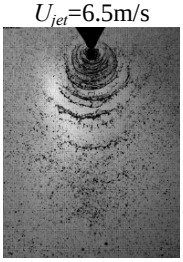 *Re*=9768 U_{jet}=9.1m/s	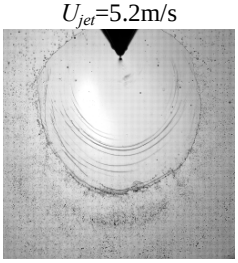 *Re*=3755 U_{jet}=9.1m/s	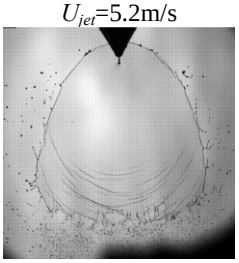 *Re*=553 U_{jet}=7.8m/s	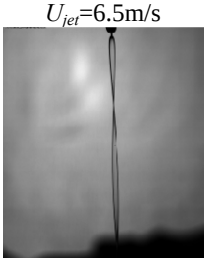 *Re*=16 U_{jet}=18.2m/s
8000	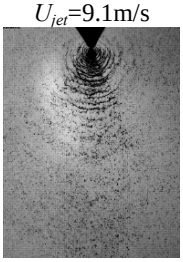 *Re*=22455 U_{jet}=20.8m/s	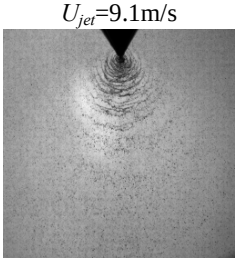 *Re*=7320 U_{jet}=16.6m/s	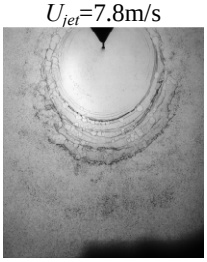 *Re*=1382 U_{jet}=19.5m/s	 *Re*=28 U_{jet}=31.2m/s
> 40000	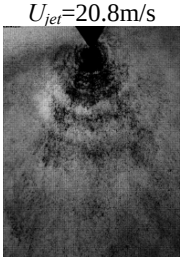 *Re*=54240 U_{jet}=49.4m/s	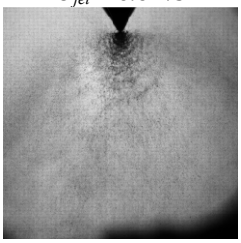 *Re*=17870 U_{jet}=42.9m/s	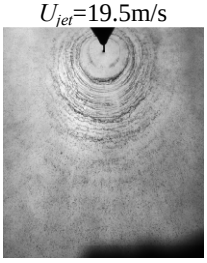 *Re*=3592 U_{jet}=50.7m/s	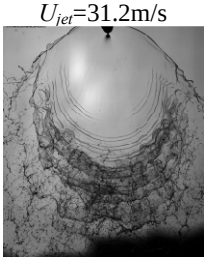 *Re*=48 U_{jet}=53.3m/s

Table 1: Breakup behaviour of 4 different fluids at increasing injection velocities

Liquid	μ [mNs/m^2]	σ [mN/m]	ρ [kg/m^3]	Oh [-] (D=0.7mm)
1-Hexene	0.252	19.00	673.0	0.0027
n-Heptane	0.387	19.65	683.6	0.0040
Water	1.002	74.00	998.0	0.0044
n-Octane	0.508	21.62	700.0	0.0049
n-Decane	0.838	23.83	730.0	0.0076
Ethanol	1.074	21.97	789.4	0.0097
30% Glycerine	2.51	71.50	1072.7	0.0108
1-Propanol	1.945	23.32	803.5	0.0170
1-Butanol	2.544	24.93	809.8	0.0214
1-Pentanol	3.619	25.36	814.4	0.0301
1-Hexanol	4.578	25.81	819.0	0.0376
1-Octanol	7.288	27.60	825.4	0.0577
Ethylene glycol	16.1	47.99	1113.0	0.0833
75% Glycerine	35.5	66.72	1192.0	0.1505
80% Glycerine	60.1	66.41	1208.5	0.2536
90% Glycerine	219	65.17	1235.1	0.9226
Triethanolamine	609	48.40	1124.2	3.1205
98% Glycerine	911	64.17	1256.4	3.8348

Table 2: List of properties of the investigated fluids. Data presented for 20°C.

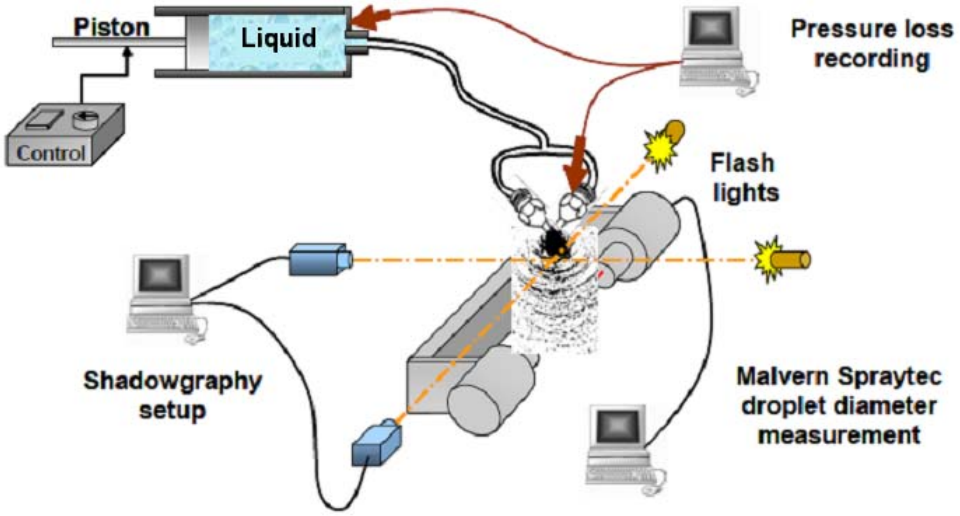

Figure 1: Experimental Setup

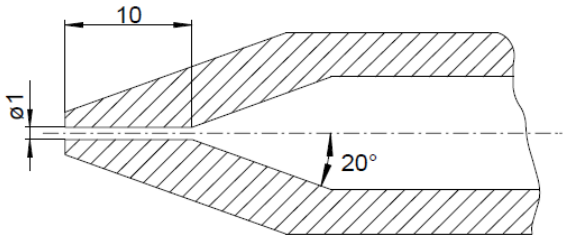

Figure 2: Injector geometry

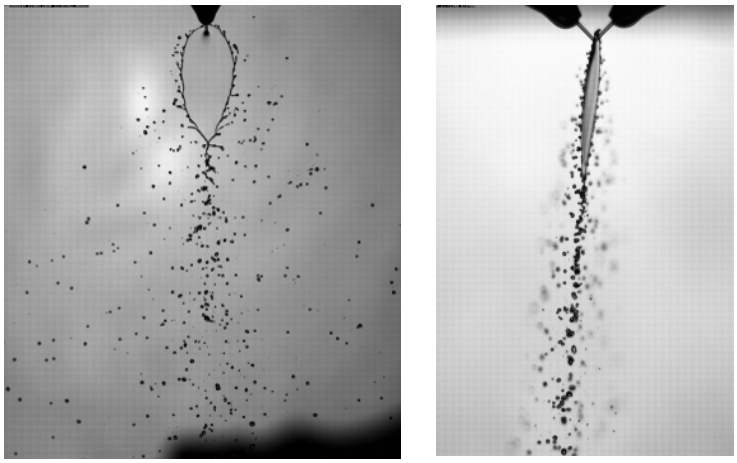

Front view Side view

Figure 3: Closed Rim: Decane (*Oh*=0.0076), U_{jet}=2.6m/s, *Re*=1316, *We*=145

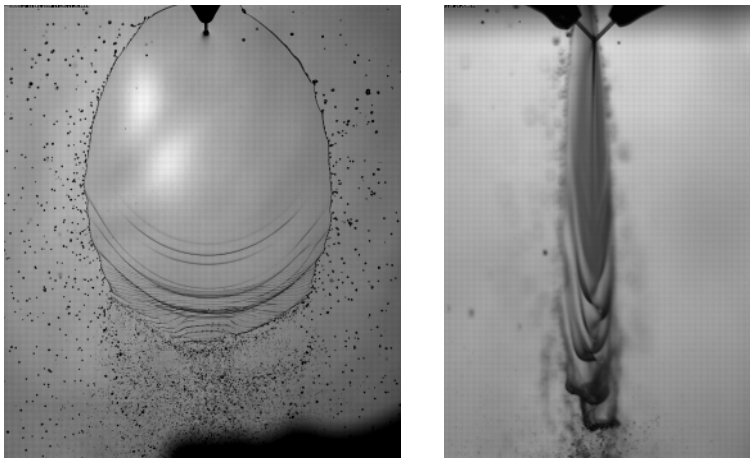

Front view Side view

Figure 4: Open Rim: Decane (*Oh*=0.0076), U_{jet}=6.5m/s, *Re*=3244, *We*=901

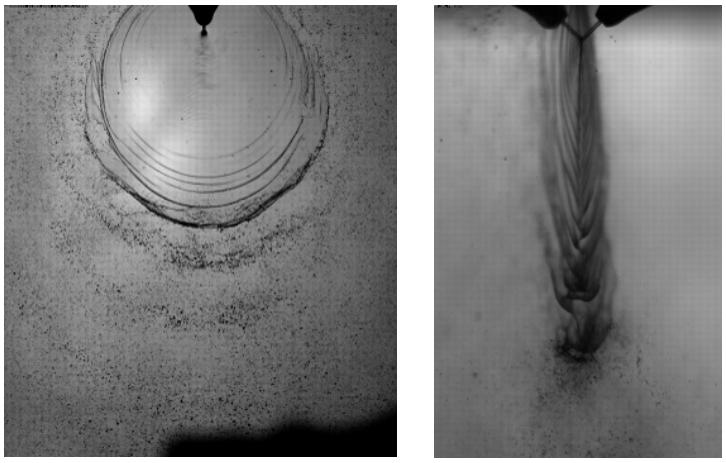

Front view Side view

Figure 5: Rimless Separation: Decane (*Oh*=0.0076), U_{jet}=9.1m/s, *Re*=4607, *We*=1772

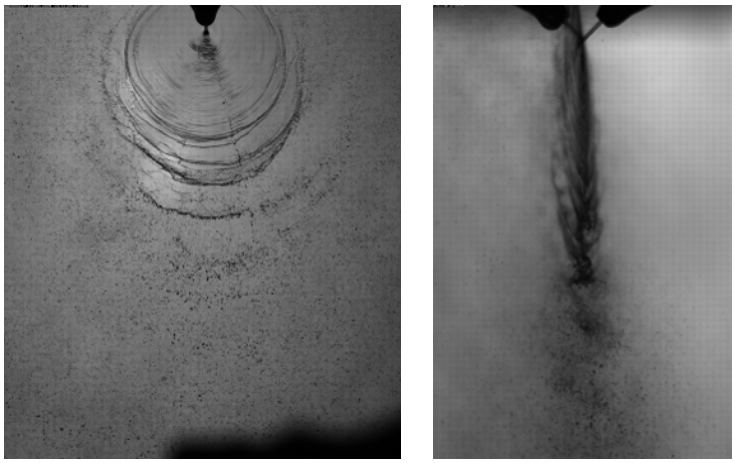

Front view Side view

Figure 6: Smooth Sheet Ligaments: Decane (Oh=0.0076), U_{jet}=2.6m/s, Re=5923, We=2930

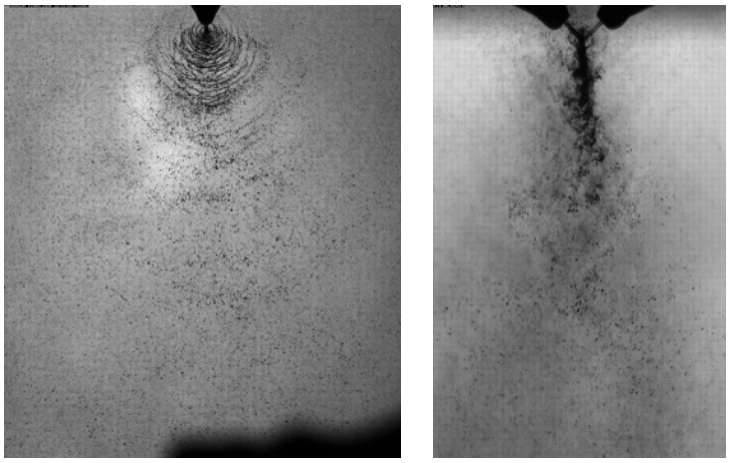

Front view Side view

Figure 7: Ruffled Sheet Ligaments: Decane (Oh=0.0076), U_{jet}=16.9m/s, Re=8617, We=6124

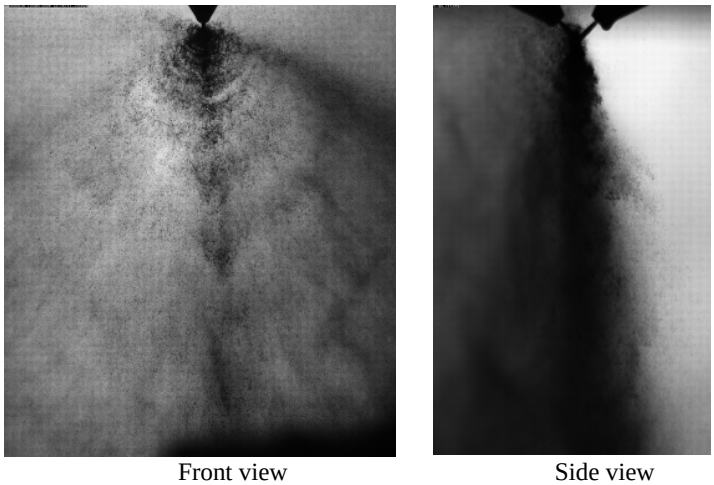

Front view Side view

Figure 8: Fully Developed Breakup: Decane (Oh=0.0076), U_{jet}=58.5m/s, Re=29405, We=73100

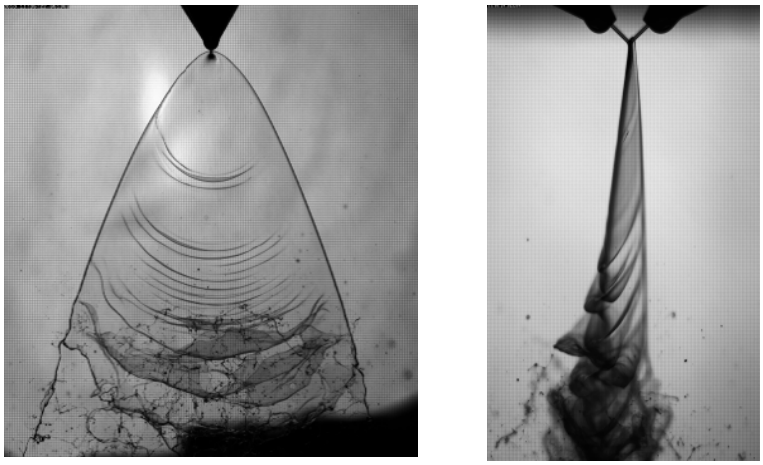

Front view Side view

Figure 9: Aerodynamic Instability Breakup: Triethanolamine (*Oh*=3.12), U_{jet}=28.6m/s, *Re*=31, *We*=13320

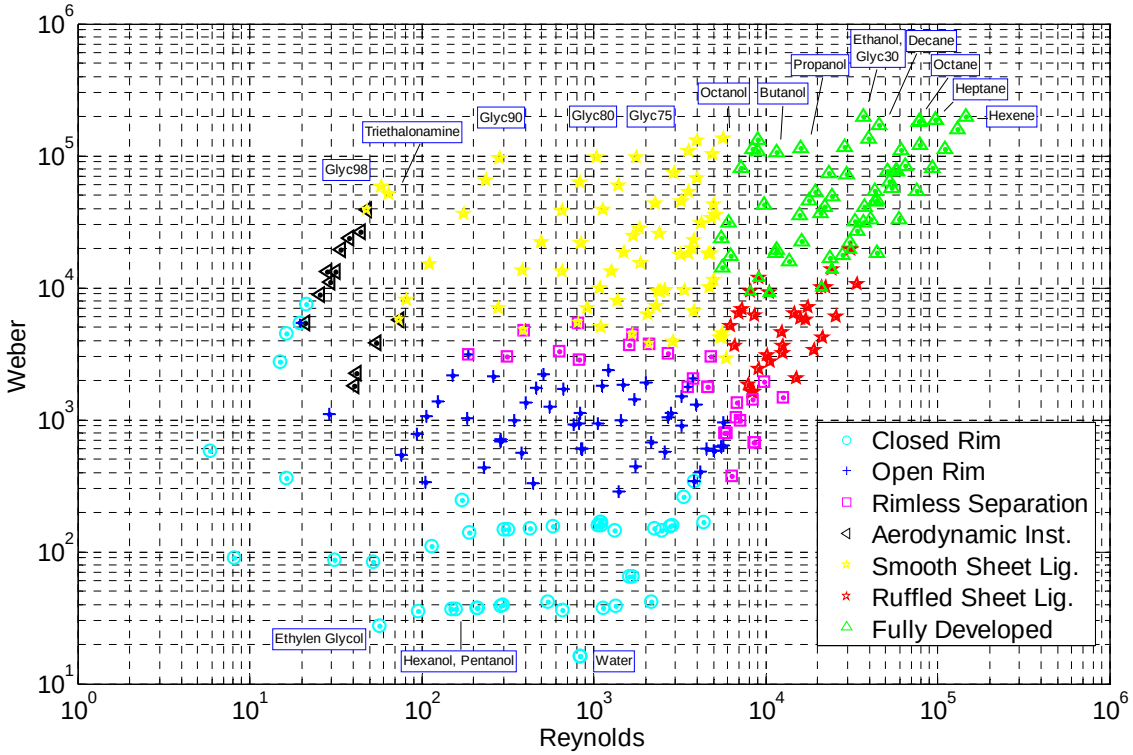

Figure 10: *Re-We* regime diagram